

*This is the post-print (i.e. final draft post-refereeing) of the publication.  
The final publication is available at AIP Publishing via <http://dx.doi.org/10.1063/5.0002983>*

## Polymorphic phase boundary in piezoelectric oxides

José Eduardo García<sup>1,a)</sup> and Fernando Rubio-Marcos<sup>2,3</sup>

<sup>1</sup>*Department of Physics, Universitat Politècnica de Catalunya - BarcelonaTech, 08034 Barcelona, Spain*

<sup>2</sup>*Department of Electroceramics, Instituto de Cerámica y Vidrio, CSIC, 28049 Madrid, Spain*

<sup>3</sup>*Escuela Politécnica Superior, Universidad Antonio de Nebrija, 28040 Madrid, Spain*

### Abstract

The design of phase boundaries has now become a consolidated strategy to improve the functional properties of piezoelectric oxides because of the unique properties that may be obtained in their vicinity. In particular, polymorphic phase boundaries (PPBs) have attracted significant interest in recent years because they represent a significant breakthrough in terms of enhanced piezoelectric activity of lead-free piezoelectric oxides. PPBs are temperature-driven phase transitions where both intrinsic and extrinsic contributions maximize, thereby enhancing the macroscopic properties of piezoelectric materials. This tutorial discusses potassium-sodium-niobate-based systems as model materials to reveal some of the most relevant advances in the design of PPBs through compositional modifications. We focus on how PPBs can be modulated by engineered doping and also discuss the direct relation between PPBs and the enhancement of piezoelectric activity. Finally, we briefly describe the main experimental techniques for detecting PPBs.

<sup>a)</sup> Author to whom correspondence should be addressed: [jose.eduardo.garcia@upc.edu](mailto:jose.eduardo.garcia@upc.edu)

## **I. INTRODUCTION**

Piezoelectric oxides, mostly perovskite-structure materials (general formula,  $ABO_3$ ), exhibit notable capacity to convert electrical energy into mechanical energy and vice versa. As functional materials, they are widely used in modern electronic devices for such things as high-precision actuation, medical ultrasonic imaging, fuel injection, printing machines, and green electric power generation.<sup>1</sup> Although these materials have long been in commercial use, emerging challenges have retained the attention of the scientific community to find new high-performance piezoelectric oxides with specific characteristics and/or functionalities. For instance, environmental concerns have led to the development of new eco-friendly piezoelectric compositions.<sup>2</sup> More recently, advances in piezoelectric technology for energy harvesting have demonstrated the need for low-cost, high-sensitivity piezoelectrics that undergo large deformations in response to low applied voltages.<sup>3</sup>

Today, the huge market of piezoelectric oxides is particularly dominated by polycrystals because polycrystalline materials are easily manufactured with reproducible properties at low cost. Although single crystals usually offer enhanced properties, they are expensive to manufacture on a large scale, which limits their commercial use.<sup>4</sup> The clear advantages of using polycrystals in piezoelectric technologies have also produced a scientific challenge because the miniaturization trend requires piezoceramics with submicron grain size.<sup>5</sup> Thus, numerous studies have focused on producing high-performance nanostructured piezoceramics.

Compositionally, the usefulness of piezoelectric oxides is mainly determined by the construction of phase boundaries between ferroelectric polymorphs.<sup>6</sup> Numerous experimental and theoretical works have investigated the relationship between phase boundaries and piezoelectric activity. The intrinsic mechanism that enhances the properties near the phase boundaries is generally accepted to be the anisotropic flattening of the free-energy profile, which is a mechanism common to most phase transitions.<sup>7-9</sup> A flat energy profile involves an easy path for varying the polarization because phase boundaries separate two phases with different polarization orientations. Therefore, both polarization rotation and polarization extension are mechanisms for improving properties that depend on the polarization variation, such as the piezoelectric response.<sup>10</sup>

Note that ferroelectric domains usually form in piezoelectric oxides to compensate the depolarization field and minimize the stress produced by cooling from the nonpolar cubic phase to the polar ferroelectric phase. Domains are regions with differing polarization orientations separated by so-called domain walls. The boundary conditions between adjacent domains depend on the crystallographic phase such that the domain configuration is often complex at phase boundaries.<sup>11</sup> Given a suitable external stimulus, domain walls can move, thereby producing a polarization variation. This extrinsic mechanism is generally the main contribution to the piezoelectric response in oxide-based piezoceramics.<sup>12</sup>

This tutorial describes a temperature-driven phase boundary, known as polymorphic phase boundary (PPB), wherein both intrinsic and extrinsic contributions are maximized. In addition, it covers the construction of PPBs in piezoelectric oxides and presents a broad overview of the experimental techniques for detecting PPBs.

## **II. POLYMORPHIC VERSUS MORPHOTROPIC PHASE BOUNDARY**

Lead zirconate titanate,  $\text{Pb}(\text{Ti,Zr})\text{O}_3$  (PZT), is surely the best known polycrystalline piezoelectric oxide because of its outstanding properties and ease of large-scale manufacturing.<sup>13,14</sup> PZT has exceptional properties for compositions in which the so-called morphotropic phase boundary (MPB) forms between the tetragonal and rhombohedral polar phases (via an intermediate monoclinic phase).<sup>6,15</sup> In general, MPBs delimit compositional-driven structural phase transitions (Fig. 1). Therefore, large polarization rotation and/or polarization extension phenomena promote the electromechanical properties enhancement of materials with MPBs.<sup>10</sup> The compositionally induced structural change is of significant practical interest because the transition driver (i.e., the composition) is maintained under working conditions. Thus, the functional properties of MPB materials are notably stable over a broad range of temperature, time, and pressure.<sup>16</sup>

The extraordinary electromechanical properties of PZT are also due to the ease with which it can be compositionally engineered, making this system adaptable to a wide range of different applications. Although PZT has been commercially undisputed for a long time, environmental concerns over its lead content have triggered an intense search for high-performance lead-free piezoelectric

materials,<sup>17–20</sup> which has focused on compositions with PZT-like MPBs. However, replacing PZT has proven to be a titanic scientific and technological challenge such that lead-based piezoelectrics, and particularly PZT, currently remain exempted as hazardous substances in electric and electronic components.

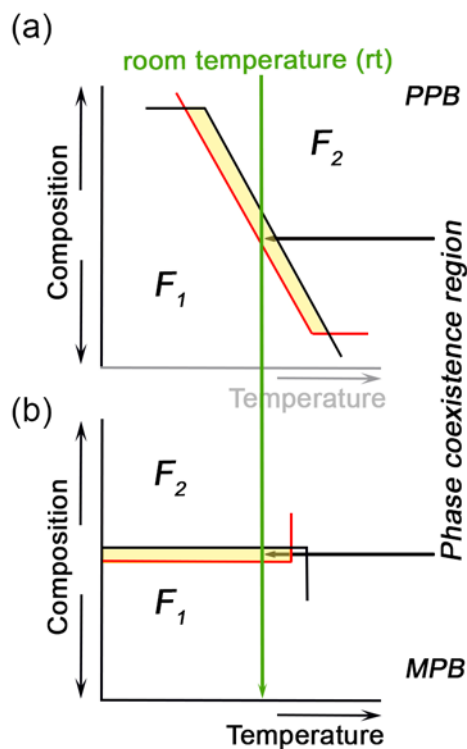


**FIG. 1.** Schematic representation of a composition-versus-temperature plot when a phase boundary exists between ferroelectric polymorphs  $F_1$  and  $F_2$  that coexist for a particular composition. (a) A polymorphic phase boundary (PPB) separates two polymorphs for a given composition over a narrow temperature range. (b) A temperature-independent morphotropic phase boundary (MPB) separates two polymorphs.

Several lead-free oxide-based solid solutions have already been intensively investigated. Among these, potassium-sodium-niobate-based materials,  $(\text{K,Na})\text{NbO}_3$  (KNN), have been enthusiastically explored because they provide a strong piezoelectric response and a relatively high depolarization (Curie) temperature for a singular KNN composition.<sup>21</sup> The surprising properties of this material originate not only in a MPB but also in a polymorphic phase boundary (PPB). From a broader perspective, PPBs are regions where a temperature-driven structural phase transition occurs (Fig. 1), which is also described as a structurally bridging low-symmetry (monoclinic) region.<sup>22</sup>

Like a MPB, the phase coexistence in a PPB favors the polarization-rotation phenomenon because the energy profile flattens in this region.<sup>23</sup> Moreover, a reversible electric-field-induced phase

transition (i.e., a polarization-extension phenomenon) is reportedly responsible for the enhanced properties in PPB regions.<sup>24</sup> Although it is generally agreed that both polarization rotation and extension (i.e., intrinsic contributions) increase upon approaching PPBs, recent results demonstrate that the extrinsic contribution to the material response is also maximized at PPBs.<sup>25</sup> In fact, an enhanced extrinsic response seems to be a universal feature in ferroelectric compositions containing phase boundaries. Note that the extrinsic contribution is defined as any response other than the intrinsic response and, in perovskite polycrystals, is mainly due to domain-wall motion.<sup>26</sup>

Designing appropriate PPBs has thus become a fundamental avenue to enhance the piezoelectric properties in numerous lead-free oxide-based piezoelectric systems, as detailed in several recent reviews.<sup>2,9,27</sup> Significant progress has been made, and excellent properties characteristics have been achieved for specific compositions. However, the major drawback of PPB-containing piezoelectrics is that their properties are temperature sensitive, which limits the use of these materials in commercial applications.

### **III. EXPERIMENTAL DETECTION OF POLYMORPHIC PHASE BOUNDARIES**

This section focuses on the detection of PPBs. Since PPBs are regions delimiting two ferroelectric phases, they can be detected by any experimental technique that resolves structural phases. Although this basic principle seems simple, in practice, an accurate determination of phase compositions at PPBs requires a careful combination of powerful analytical tools.

#### **A. X-ray diffraction**

X-ray diffraction (XRD) is a well-known technique that is widely used in materials science to identify structural phases. Temperature-dependent XRD measurements provide information about phase transformations bridged through a PPB (Fig. 2).<sup>25</sup> An advanced analysis is possible by using high-resolution synchrotron XRD, which gives precise information on the phase composition and reveals intermediate phases that may coexist in PPBs.<sup>28,29</sup>

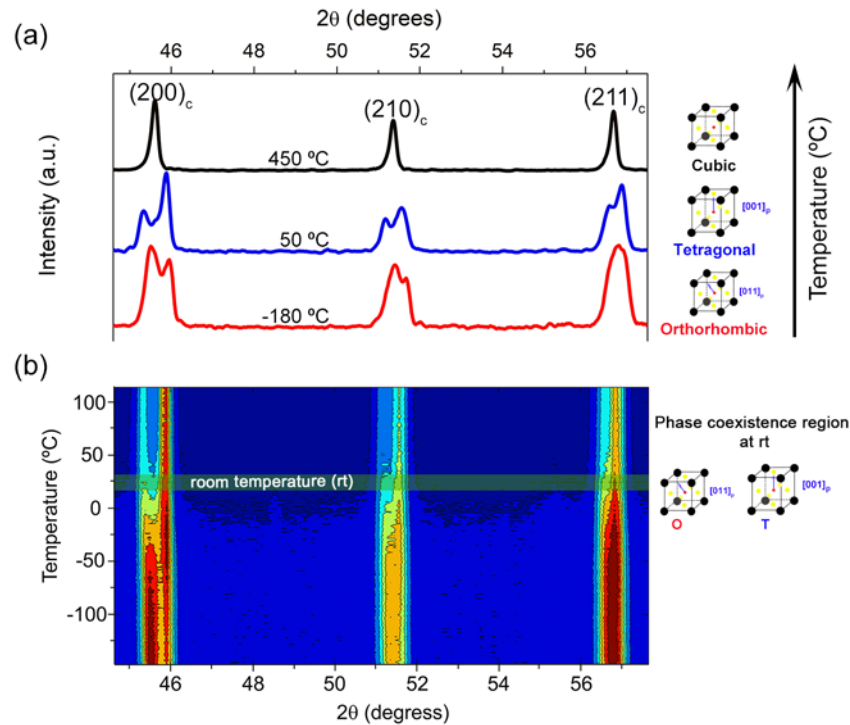


**FIG. 2.** Temperature-dependent x-ray diffraction (XRD) results for  $(\text{K}_{0.44}\text{Na}_{0.52}\text{Li}_{0.04})(\text{Nb}_{0.86}\text{Ta}_{0.10}\text{Sb}_{0.06})\text{O}_3$  (KNL-NTS). (a) XRD one-dimensional patterns for KNL-NTS reveal different crystallographic phases at three representative temperatures. A cubic phase and an orthorhombic phase appear at high and low temperatures, respectively, and a tetragonal phase is detected slightly above room temperature. (b) A contour plot reveals clearly the existence of a room-temperature orthorhombic-tetragonal PPB region, where the width and intensity of the reflection lines change as the sample goes from the orthorhombic phase to the tetragonal phase.

## B. Dielectric response

The temperature dependence of the dielectric response provides a relatively simple experimental method to reveal PPBs. The real ( $\epsilon'$ ) and imaginary ( $\epsilon''$ ) permittivity versus temperature ( $T$ ) plots show a local maximum when a phase transformation occurs, as is observed on the well-known  $\epsilon'(T)$  plot of barium titanate.<sup>30</sup> PPBs cause similar, but broader, local maxima in  $\epsilon'(T)$  and  $\epsilon''(T)$  plots (Fig. 3), which constitutes a useful, low-cost method to examine, for instance, how a compositional modification shifts the PPB region.

Note that dielectric measurements are useful only when PPB region is expected to be appeared, because local maximum in permittivity-versus-temperature plot may emerge as a result of phenomena other than phase transformations, such as relaxation processes.<sup>31–33</sup>

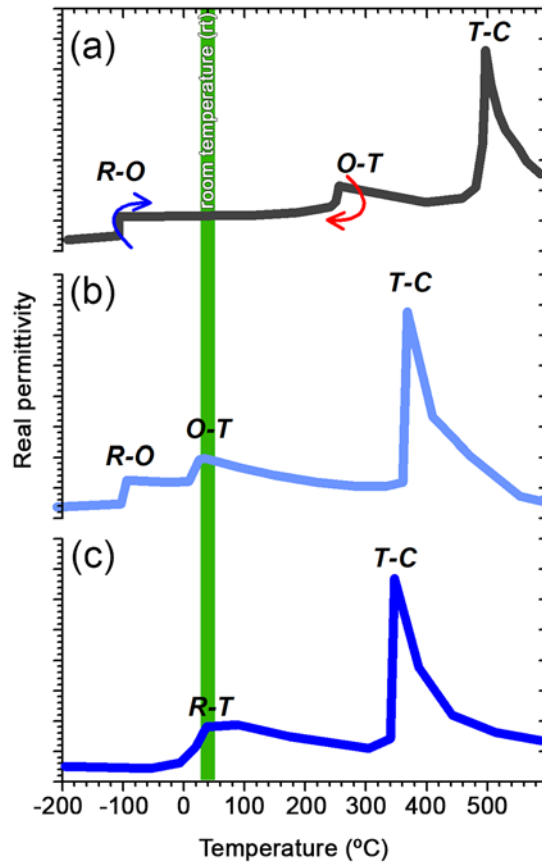


**FIG. 3.** Schematic representation of temperature dependence of real permittivity ( $\epsilon'$ ) in potassium-sodium-niobate-based (KNN-based) systems. Four polymorphic phases, rhombohedral (R), orthorhombic (O), tetragonal (T), and cubic (C), appear in this system as the temperature increases. The phase changes are revealed as local maxima in the  $\epsilon'$ - $T$  plots. (a) Unmodified  $(\text{K}_{0.5}\text{Na}_{0.5})\text{NbO}_3$  shows the R-O and O-T phase transformations below and above room temperature, respectively, whereas the T-C phase transition occurs at high temperature. (b) The O-T phase boundary shifts to room temperature upon appropriate substitution at the (K, Na) and/or Nb sites by isovalent cations. This effect is usually accompanied by a decrease in the T-C transition temperature. (c) An appropriate choice of additives and their concentration suppresses the O-T boundary in favor of the R-T phase boundary.

### C. Other experimental techniques

As stated above, all experimental techniques that detect polar phases may be used to characterize PPB regions. Thus, Raman spectroscopy, transmission electron microscopy, neutron diffraction, and other techniques may also be considered. For instance, the results of Raman spectroscopy of KNN-based systems indicate that the vibrations of  $\text{NbO}_6$  octahedrons are sensitive to phase transitions. Therefore, the temperature dependence of the wavenumber of the double-degenerate symmetric O–Nb–O stretching vibration mode gives useful information about the structure around a PPB.<sup>34,35</sup>

#### **IV. PIEZOELECTRIC MATERIALS WITH POLYMORPHIC PHASE BOUNDARY**

From a functional perspective, the design and control of PPBs have been used to significantly enhance the piezoelectric activity of lead-free piezoelectric oxides. In this context, extensive research has focused on constructing PPBs in lead-free compounds to emulate high-performance PZT materials with MPB.<sup>9,27</sup> Consequently, KNN-based systems are discussed here as model materials to evince some of the most relevant advances in the design of PPBs through compositional modifications. Some practical aspects in the design of the most renowned PPBs in KNN piezoceramics systems are highlighted. Note that the most significant breakthrough concerning the piezoelectric properties of KNN via compositional design has been achieved by the stabilization of a rhombohedral–tetragonal phase boundary,<sup>27,36</sup> which shifts both the classical rhombohedral–orthorhombic and orthorhombic–tetragonal transitions near to room temperature [see Fig. 3(c)]. Special emphasis is placed on the coupling between phase boundaries and piezoelectric activity and on how PPBs may be modulated by engineered doping.

##### **A. Orthorhombic-tetragonal phase boundary**

Interest in PPBs was triggered by the well-known work of Saito *et al.*<sup>21</sup> in 2004, who obtained a large piezoelectric response from a KNN system by a complex simultaneous substitution into both the A and B sites of the perovskite lattice, revealing the coexistence of tetragonal (T) and orthorhombic symmetries (O) at room temperature for a given composition. Their work introduced a processing route for producing textured polycrystals that triggered research to obtain lead-free piezoceramics with similar properties without requiring special processing but taking advantage of the benefits of the O-T PPB.

From a broader perspective, chemical modifications of KNN-based materials enable the fabrication of PPBs with tailored functional characteristics, thereby providing control over the physical properties of the resulting materials. Over the last 15 years, most efforts have focused on the selective replacement of the elements forming the (K, Na)NbO<sub>3</sub>-based perovskite structure; that is, substitution into the (K, Na) and Nb sites by the elements with the same valence and similar ionic



radius. Thus, the design of O-T phase boundaries in KNN-based materials involved selective substitutions that improved the piezoelectric response of these materials.<sup>9,27</sup>

The substitution of  $\text{Li}^+$  and/or  $\text{Ag}^+$  into (K, Na) sites produces the most prominent modulation of the O-T boundary [Fig. 3(b)].<sup>34</sup> Both substitutions shift the O-T boundary close to room temperature, facilitating the polarization process, which results in a significant piezoelectric response. Intriguing features appear in relation to the physical mechanism responsible for the stabilization of the O-T boundary near room temperature. For instance, the (K, Na) site-selective replacement provokes a structural instability related to the tetragonal phase, which increases as  $\text{Li}^+$  and/or  $\text{Ag}^+$  cations are incorporated into the perovskite lattice.<sup>9,37,38</sup> This instability originates from the competition of  $\text{Li}^+$  and/or  $\text{Ag}^+$  cations with  $\text{Na}^+$  and  $\text{K}^+$  at the A site of the perovskite to form a new solid solution and strongly distorting the lattice, thereby transforming the structure from orthorhombic to tetragonal symmetry. Note that, although the ionic radii of  $\text{Li}^+$  and  $\text{Ag}^+$  are similar to those of  $\text{Na}^+$  and  $\text{K}^+$ , the former are clearly smaller.<sup>39</sup> From a practical point of view, therefore,  $T_{\text{O-T}}$  decreases, which results in the formation of room-temperature O-T PPBs.

A similar strategy based on substitution of isovalent additives into the  $\text{Nb}^{5+}$  site has also been widely used to modify the O-T boundary in the KNN system, with the most outstanding substitutions being by  $\text{Sb}^{5+}$  and/or  $\text{Ta}^{5+}$  cations.<sup>9,40,41</sup> In general, substitution into the B site decreases the  $T_{\text{O-T}}$  phase and, simultaneously, increases the  $T_{\text{R-O}}$  phase depending on the additive and its concentration (e.g., substitution by  $\text{Sb}^{5+}$  more strongly affects the phase transition than substitution by  $\text{Ta}^{5+}$ ). Note that some limitations apply to substitution into the B site; for instance, (i) reduction of the Curie temperature, (ii) the generation of compositional inhomogeneity (i.e., the inhomogeneous distribution of  $\text{Nb}^{5+}$ ,  $\text{Ta}^{5+}$ , and  $\text{Sb}^{5+}$ ), which is rather difficult to avoid because of the phase segregation of end members over a wide temperature range, and (iii) the high cost of producing  $\text{Ta}^{5+}$ . These facts imply that, in general, substitution into the B site is accompanied by simultaneous substitution into the A site (i.e., a co-substitution strategy), with the combinations  $\text{Li}^+\text{-Sb}^{5+}$ ,  $\text{Li}^+\text{-Ta}^{5+}$ , and  $\text{Li}^+\text{-Sb}^{5+}/\text{Ta}^{5+}$  being the most used because they do not reduce the Curie temperature.<sup>9,37</sup>

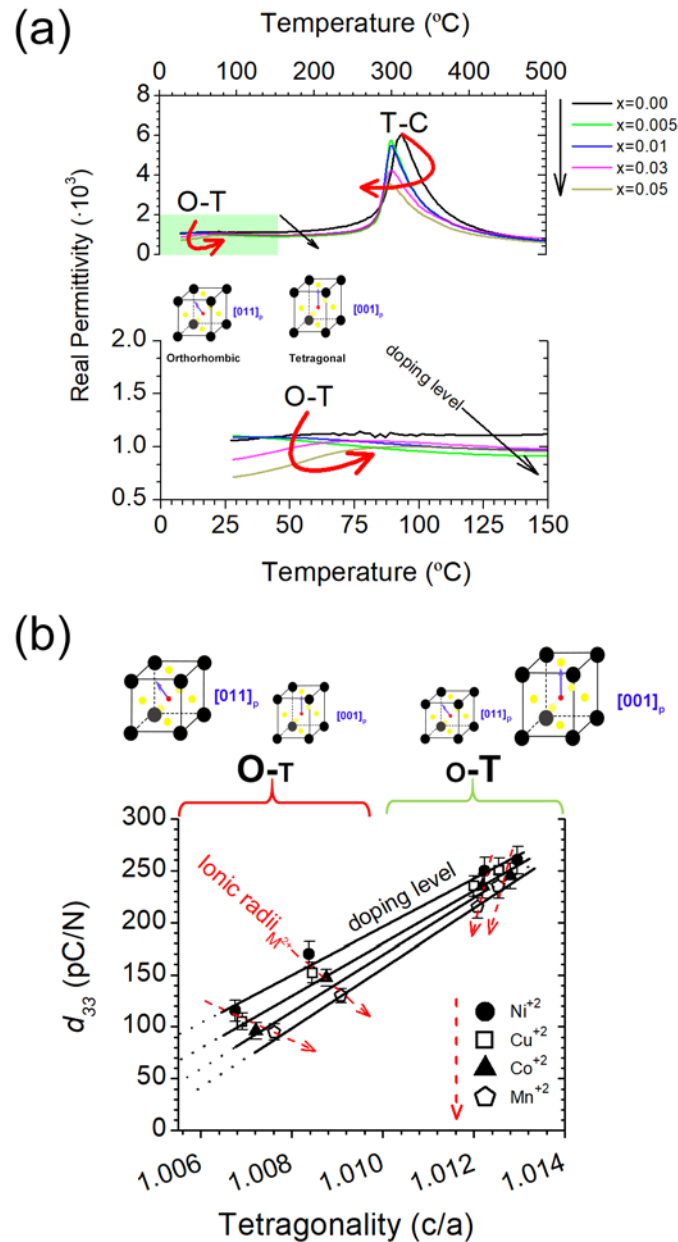


**FIG. 4.** Effect of compositional modifications induced by doping with a transition-metal oxide,  $MO$  ( $M^{2+} = \text{Ni}^{2+}, \text{Cu}^{2+}, \text{Co}^{2+}, \text{or Mn}^{2+}$ ) on O-T phase boundary of  $(\text{K}_{0.44}\text{Na}_{0.52}\text{Li}_{0.04})_{1-x}\text{M}_{x/2}(\text{Nb}_{0.86}\text{Ta}_{0.10}\text{Sb}_{0.04})\text{O}_3$  system, abbreviated as  $(\text{KNL})_{1-x}\text{M}_{x/2}\text{-NTS}$ . As a representative example, panel (a) shows the real permittivity versus temperature for  $(\text{KNL})_{1-x}\text{M}_{x/2}\text{-NTS}$  (at 100 kHz), for  $M^{2+} = \text{Co}^{2+}$  where  $0 \leq x \leq 0.05$ . The upper red arrows correspond to the evolution of the  $T_{\text{O-T}}$  and  $T_{\text{C}}$  phases, and the lower arrows correspond to the evolution of the  $T_{\text{O-T}}$  phase for different doping levels. (b) Piezoelectric coefficient  $d_{33}$  as a function of tetragonality ratio  $c/a$  for  $(\text{KNL})_{1-x}\text{M}_{x/2}\text{-NTS}$  ceramics for several metal ions  $M^{2+}$ . Note that the doping strategy with  $M^{2+}$  transition elements in the  $(\text{KNL})_{1-x}\text{M}_{x/2}\text{-NTS}$  system produces two different behaviors depending on the doping level and ionic radii. At low doping level, the T polymorph is most relevant because it has greater tetragonality. In contrast, for compositions with high  $M^{2+}$  content ( $0.03 \leq x \leq 0.05$ ), the O polymorph, which involves the stabilization of orthorhombic symmetry, becomes more relevant.

Historically, engineered doping has been widely used to modulate the functional properties of various materials. For KNN-based systems, doping is often used to form point defects and thereby tailor the electrical properties of the material; however, the O-T phase boundary is also modified. Of the possible additives (or doping elements), many aliovalent compositional modifications have been studied with ions of either higher valence (donors) or lower valence (acceptors).<sup>38</sup> Three approaches have been widely reported: selective modification of either the A or B site by aliovalent metals and, more importantly, the simultaneous modification of both the A and B sites. Depending on the ionic radius of the dopants, some of the selected additives could be substituted into either the A or B site.

In this regard, the modifications induced by doping with transition-metal oxides  $MO$  ( $M^{2+} = \text{Ni}^{2+}$ ,  $\text{Cu}^{2+}$ ,  $\text{Co}^{2+}$ , and  $\text{Mn}^{2+}$ ),<sup>42-45</sup> at the O-T phase boundary are highlighted below as illustrative examples (Fig. 4). As mentioned before, the selected  $M^{2+}$  ion could, depending on its ionic radius, substitute into either the A or B site. Consequently, taking into account its valency,  $M^{2+}$  can act either as a donor-dopant (if introduced into an A site) or as an acceptor-dopant (if introduced into a B site). Therefore, doping KNN-based systems by  $M^{2+}$  produces two different behaviors. From both perspectives (i.e., doping level and ionic radii), the room-temperature stabilization of the O-T boundary at low doping levels is tentatively associated with doping by  $M^{2+}$  donors [Fig. 4(a)], with a slight reduction with increasing ionic radius of the dopant. This behavior can be explained by noting that the  $M^{2+}$  ions may occupy the A sites (donor-type doping), which causes lattice slack, thereby shifting  $T_{\text{O-T}}$  closer to room temperature. Moreover, the simultaneous motion of  $90^\circ$  and  $180^\circ$  domains due to the stabilization near room temperature of the O-T phase boundary stabilizes the piezoelectric properties [Fig. 4(b)]. In contrast, for a high doping range, the system becomes orthorhombic, and an increased ionic radius increases  $T_{\text{O-T}}$  [Fig. 4(a)]. In this case, the solubility of  $M^{2+}$  ions in the perovskite lattice seems rather limited, which gives rise to a secondary phase that may be assigned to a tetragonal tungsten-bronze-type structure. Furthermore,  $M^{2+}$  ions substitute into the B site, exhibiting some properties of acceptor-type additives. Thus, piezoelectric properties are degraded [Fig. 4(b)].

## **B. Rhombohedral–tetragonal phase boundary**

Since 2013, research into the design of polymorphic phase boundaries has turned toward the stabilization of a new room-temperature rhombohedral–tetragonal (R-T) phase boundary.<sup>27</sup> The room-temperature stabilization of a R-T phase boundary is revealed mainly by the high degree of polarization directions the system exhibits at room temperature, which is associated with the polarization direction along the  $[001]_p$  and  $[111]_p$  primitive-cell edges for the R and T phases, respectively. The coexistence of the R and T phases contributes to the domain-wall mobility and therefore to the enhanced piezoelectric properties at room temperature.

In analogy with the above, this section presents details about the main strategies for stabilizing the rhombohedral–tetragonal phase boundary in KNN-based systems by compositional design. Generally speaking, the construction of a rhombohedral–tetragonal phase boundary is governed by an appropriate choice of additives and the control of their concentrations.<sup>27</sup> By tailoring the additive content, the O-T boundary can be suppressed in favor of a new R-T phase boundary. To illustrate this, Fig. 5 shows the construction of a rhombohedral–tetragonal PPB in KNN-based ceramics. As expected, the system is clearly polymorphic at room temperature because of the coexistence between tetragonal and orthorhombic or rhombohedral symmetries modulated by the additive content [Fig. 5(a)]. The O-T phases coexist for compositions with  $0.00 \leq x \leq 0.06$  (where  $x$  is the doping concentration), which is more relevant to the peaks associated with T symmetry.<sup>46</sup> In contrast, the compositional range  $0.07 \leq x \leq 0.08$  produces a mixed R-T phase structure. The temperature dependence of the permittivity [Figs. 5(b) and 5(c)] further confirms the stabilization close to room temperature of the R-T phase boundary. As the dopant concentration increases,  $T_{O-T}$  reduces whereas  $T_{R-O}$  increases, which stabilizes the R-T phase boundary when the O-T boundary disappears. As expected, the stabilization of PPBs plays a crucial role in the functional properties of the system.<sup>46</sup> Figure 5(d) shows the evolution of  $d_{33}$  for O-T and R-T phase boundaries, revealing that the O-T phase boundary ( $0.00 \leq x \leq 0.06$ ) increases  $d_{33}$ , which reaches a maximum of  $\sim 315 \text{ pC N}^{-1}$  at  $x = 0.06$ . In addition,  $d_{33}$  is substantially enhanced near the R-T phase boundary, reaching a maximum of  $\sim 400 \text{ pC} \cdot \text{N}^{-1}$  at  $x = 0.07$ .

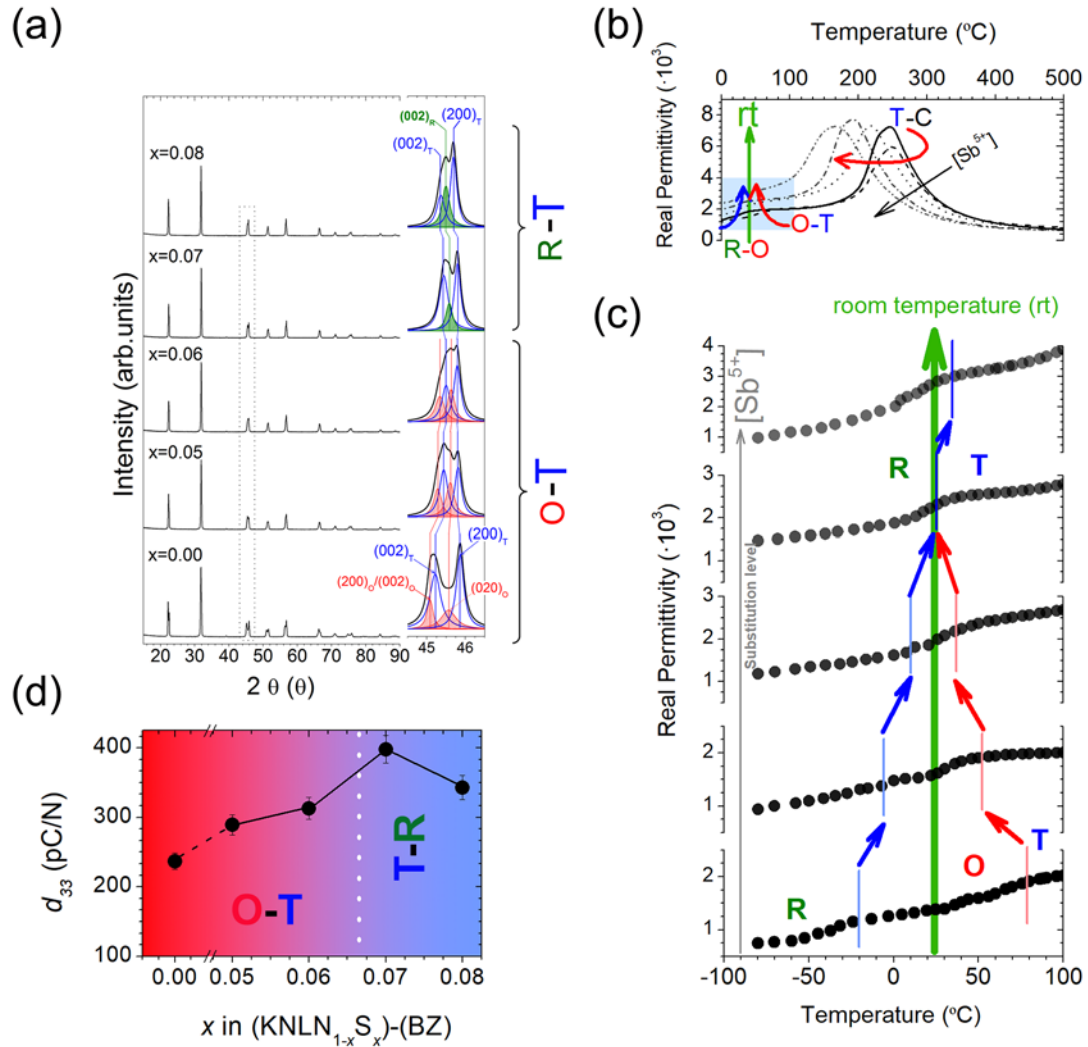


**FIG. 5.** Systematic study of the effects of compositional design by selective substitution into the B sites with  $\text{Sb}^{5+}$  ions in  $0.96[(\text{K}_{0.48}\text{Na}_{0.52})_{0.95}\text{Li}_{0.05}\text{Nb}_{1-x}\text{Sb}_x\text{O}_3]-0.04[\text{BaZrO}_3]$  lead-free piezoceramics ( $\text{KNLN}_{1-x}\text{S}_x\text{-BZ}$ ). (a) The coexistence between a tetragonal symmetry (T,  $P4mm$ ), an orthorhombic symmetry (O,  $\text{Amm}2$ ), and a rhombohedral symmetry (R,  $\text{R}3c$ ) is identified from inspecting the x-ray diffraction pattern. (b) Real permittivity ( $\epsilon'$ ) versus temperature of  $\text{KNLN}_{1-x}\text{S}_x\text{-BZ}$  at 100 kHz. The red arrows in panel (a) indicate the  $T_{\text{O-T}}$  and  $T_{\text{C}}$  evolution, whereas the blue arrows indicate the  $T_{\text{R-O}}$  evolution depending on the  $\text{Sb}^{5+}$  content. Panel (c) shows a detail of the  $\epsilon'\text{-T}$  curves in the temperature range  $-80$  to  $100$   $^{\circ}\text{C}$ , where two situations can be identified depending on the doping content. For low doping, the material have O-T phase coexistence near room temperature whereas, for high doping, the O-T phase boundary is suppressed in favor of a new R-T phase transition. Panel (d) shows how the O-T and R-T phase boundaries affect the  $d_{33}$  value at room temperature, suggesting that the piezoelectric properties of the system can be enhanced by modifying the phase coexistence and the relative volume fraction of each polymorph.

The existence of an intermediate state between both O-T and R-T phase boundary was recently demonstrated and shows that an R-O-T multiphase coexists with diffuse behavior.<sup>27,29,47,48</sup> The R-O-T phase boundary was produced in the KNN system, showing that it is mainly composed of the O and T phases, whereas the R phase is present but in the form of a “diffuse” phase.<sup>48</sup> This approach

was used on materials with high piezoelectric response ( $d_{33} = 400\text{--}650$  pC/N), enhanced strain response, and superior temperature stability.

Finally, note that PPBs behave similarly with regard to the phase ratio of the system. Thus, research indicates that both the phase ratio and the tetragonality (as indicated by the  $c/a$  ratio) determine the functional properties—in particular, the piezoelectric response [Fig. 4(b)].<sup>27,49,50</sup> Thus, a larger tetragonality ratio combined with a higher relative volume fraction of the T phase produces superior piezoelectric response.

## **V. SUMMARY AND OUTLOOK**

As discussed above, piezoelectric oxides with PPBs have attracted significant attention because of their potential for use as high-performance lead-free piezoceramics. PPBs are regions where two ferroelectric polymorphs coexist and both polarization variation and domain-wall motion are maximized. The major drawback of PPBs is that they include regions where a temperature-driven structural phase transition occurs, which means that the functional properties around PPBs are often thermally unstable. However, significant efforts are being made to obtain materials with thermally stable piezoelectric properties by constructing new PPBs through compositional design.

Given that dopants strongly affect the phase ratio forming PPBs, engineered doping has proven to be a useful tool to tune the functional properties of these materials. Although the physical mechanisms responsible for the enhanced piezoelectric properties associated with PPBs should be further studied, the stabilization of a rich tetragonal region in PPBs seems to be crucial for improving the piezoelectric activity. Thus, although more efforts are needed for these materials to enter industrial applications, PPB oxide-based lead-free materials now offer a realistic alternative to lead-based materials.

## **ACKNOWLEDGMENTS**

The authors gratefully acknowledge the support of the AEI (Spanish Government) projects MAT2017-86450-C4-1-R and PGC2018-099158-B-I00. F.R.-M. is indebted to MINECO for a “Ramon y Cajal” contract (ref: RyC-2015-18626), which is co-financed by the European Social

Fund. F.R.-M. also acknowledges support from a 2018 Leonardo Grant for Researchers and Cultural Creators, BBVA Foundation.

## REFERENCES

- <sup>1</sup> J. Hao, W. Li, J. Zhai, and H. Chen, *Mater. Sci. Eng. R-Rep.* **135**, 1 (2019).
- <sup>2</sup> T. Zheng, J. Wu, D. Xiao, and J. Zhu, *Prog. Mater. Sci.* **98**, 552 (2018).
- <sup>3</sup> H. Liu, J. Zhong, C. Lee, S.-W. Lee, and L. Lin, *Appl. Phys. Rev.* **5**, 041306 (2018).
- <sup>4</sup> S. Zhang and F. Li, *J. Appl. Phys.* **111**, 031301 (2012).
- <sup>5</sup> P. Muralt, *J. Am. Ceram. Soc.* **91**, 1385 (2008).
- <sup>6</sup> R. Guo, L. E. Cross, S-E. Park, B. Noheda, D. E. Cox, and G. Shirane, *Phys. Rev. Lett.* **84**, 5423 (2000).
- <sup>7</sup> H. Fu and R. E. Cohen, *Nature (London)* **403**, 281 (2000).
- <sup>8</sup> D. Damjanovic, *J. Am. Ceram. Soc.* **88**, 2663 (2005).
- <sup>9</sup> J. Wu, D. Xiao, and J. Zhu, *Chem. Rev.* **115**, 2559 (2015).
- <sup>10</sup> D. Damjanovic, *Appl. Phys. Lett.* **97**, 062906 (2010).
- <sup>11</sup> G. Catalan, J. Seidel, R. Ramesh, and J. F. Scott, *Rev. Mod. Phys.* **84**, 119 (2012).
- <sup>12</sup> J. E. Garcia, *Materials* **8**, 7821 (2015).
- <sup>13</sup> G. H. Haertling, *J. Am. Ceram. Soc.* **82**, 797 (1999).
- <sup>14</sup> T. R. Shrout and S. J. Zhang, *J. Electroceram.* **19**, 111 (2007).
- <sup>15</sup> B. Noheda, D. E. Cox, and G. Shirane, *Appl. Phys. Lett.* **74**, 2059 (1999).
- <sup>16</sup> D. Damjanovic, *Rep. Prog. Phys.* **61**, 1267 (1998).
- <sup>17</sup> J. Rödel, W. Jo, K. T. P. Seifert, E.-M. Anton, T. Granzow, and D. Damjanovic, *J. Am. Ceram. Soc.* **92**, 1153 (2009).
- <sup>18</sup> J. Rödel, K. G. Webber, R. Dittmer, W. Jo, M. Kimura, and D. Damjanovic, *J. Eur. Ceram. Soc.* **35**, 1659 (2015).
- <sup>19</sup> C.-H. Hong, H.-P. Kim, B.-Y. Choi, H.-S. Han, J. S. Son, C. W. Ahn, and W. Jo, *J. Materiomics* **2**, 1 (2016).
- <sup>20</sup> J. Koruza, A. J. Bell, T. Fromling, K. G. Webber, K. Wang, and J. Rödel, *J. Materiomics* **4**, 13 (2018).
- <sup>21</sup> Y. Saito, H. Takao, T. Tani, T. Nonoyama, K. Takatori, T. Homma, T. Nagaya, and M. Nakamura, *Nature (London)* **432**, 84 (2004).
- <sup>22</sup> W. Ge, Y. Ren, J. Zhang, C. P. Devreugd, J. Li, and D. Viehland, *J. Appl. Phys.* **111**, 103503 (2012).

- <sup>23</sup> J. Gao, S. Ren, L. Zhang, Y. Hao, M. Fang, M. Zhang, Y. Dai, X. Hu, D. Wang, L. Zhong, S. Li, and X. Ren, *Appl. Phys. Lett.* **107**, 032902 (2015).
- <sup>24</sup> T. Iamsasri, G. Tutuncu, C. Uthaisar, S. Wongsanmai, S. Pojprapai, and J. L. Jones, *J. Appl. Phys.* **117**, 024101 (2015).
- <sup>25</sup> D. A. Ochoa, G. Esteves, J. L. Jones, F. Rubio-Marcos, J. F. Fernandez, and J. E. Garcia, *Appl. Phys. Lett.* **108**, 142901 (2016).
- <sup>26</sup> Q. M. Zhang, H. Wang, N. Kim, and L. E. Cross, *J. Appl. Phys.* **75**, 454 (1994).
- <sup>27</sup> X. Lv, J. Zhu, D. Xiao, X. Zhang, and J. Wu, *Chem. Soc. Rev.* **49**, 671 (2020).
- <sup>28</sup> J. Fu, R. Zuo, S. C. Wu, J. Z. Jiang, L. Li, T. Y. Yang, X. Wang, and L. Li, *Appl. Phys. Lett.* **100**, 122902 (2012).
- <sup>29</sup> F.-Z. Yao, K. Wang, W. Jo, K. G. Webber, T. P. Comyn, J.-X. Ding, B. Xu, L.-Q. Cheng, M.-P. Zheng, Y.-D. Hou, and J.-F. Li, *Adv. Funct. Mater.* **26**, 1217 (2016).
- <sup>30</sup> V. Buscaglia and C. A. Randall, *J. Eur. Ceram. Soc.* DOI: 10.1016/j.jeurceramsoc.2020.01.021.
- <sup>31</sup> J. E. Garcia, V. Gomis, R. Perez, A. Albareda, and J. A. Eiras, *Appl. Phys. Lett.* **91**, 042902 (2007).
- <sup>32</sup> D. A. Ochoa, J. E. Garcia, R. Perez, V. Gomis, A. Albareda, F. Rubio-Marcos, and J. F. Fernandez, *J. Phys. D* **42**, 025402 (2009).
- <sup>33</sup> D. A. Ochoa, R. Levit, C. M. Fancher, G. Esteves, J. L. Jones, and J. E. García, *J. Phys. D* **50**, 205305 (2017).
- <sup>34</sup> Y. Dai, X. Zhang, and G. Zhou, *Appl. Phys. Lett.* **90**, 262903 (2007).
- <sup>35</sup> T. Zheng, H. Wu, Y. Yuan, X. Lv, Q. Li, T. Men, C. Zhao, D. Xiao, J. Wu, K. Wang, J.-F. Li, Y. Gu, J. Zhu, and S. J. Pennycook, *Energy Environ. Sci.* **10**, 528 (2017).
- <sup>36</sup> B. Zhang, J. Wu, X. Cheng, X. Wang, D. Xiao, J. Zhu, X. Wang and X. Lou, *ACS Appl. Mater. Interfaces* **5**, 7718 (2013).
- <sup>37</sup> J. F. Li, K. Wang, F. Y. Zhu, L. Q. Cheng and F. Z. Yao, *J. Am. Ceram. Soc.* **96**, 3677 (2013).
- <sup>38</sup> Y. Zhang and J.-F. Li, *J. Mater. Chem. C* **7**, 4284 (2019).
- <sup>39</sup> R. D. Shannon, *Acta Crystallogr. A* **32**, 751 (1976).
- <sup>40</sup> R. Zuo, J. Fu, D. Lv and Y. Liu, *J. Am. Ceram. Soc.* **93**, 2783 (2010).
- <sup>41</sup> Y. G. Lv, C. L. Wang, J. L. Zhang, L. Wu, M. L. Zhao, and J. P. Xu, *Mater. Res. Bull.* **44**, 284 (2009).
- <sup>42</sup> F. Rubio-Marcos, P. Marchet, J. J. Romero, and J.F. Fernández, *J. Eur. Ceram. Soc.* **31**, 2309 (2011).



- <sup>43</sup> F. Rubio-Marcos, J. J. Reinoso, X. Vendrell, J. J. Romero, L. Mestres, P. Leret, J. F. Fernández, and P. Marchet, *Ceram. Int.* **39**, 4139 (2013).
- <sup>44</sup> F. Rubio-Marcos, P. Marchet, J. R. Duclere, J. J. Romero, and J. F. Fernandez, *Solid State Commun.* **151**, 1463 (2011).
- <sup>45</sup> F. Rubio-Marcos, P. Marchet, X. Vendrell, L. Mestres, J. J. Romero, R. Rémondier, and J. F. Fernández, *J. Alloy. Compd.* **509**, 8804 (2011).
- <sup>46</sup> F. Rubio-Marcos, R. López-Juárez, R. E. Rojas-Hernandez, A. Del Campo, N. Razo-Pérez, and J. F. Fernandez, *ACS Appl. Mater. Interfaces* **7**, 23080 (2015).
- <sup>47</sup> Q. Liu, Y. Zhang, J. Gao, Z. Zhou, H. Wang, K. Wang, X. Zhang, L. Li, and J.-F. Li, *Energy Environ. Sci.* **11**, 3531 (2018).
- <sup>48</sup> X. Sun, J. Zhang, X. Lv, Y. Liu, F. Li, and J. Wu, *J. Mater. Chem. A* **7**, 16803 (2019).
- <sup>49</sup> X. Lv, J. Wu, J. Zhu, D. Xiao, and X. Zhang, *J. Eur. Ceram. Soc.* **38**, 85 (2017).
- <sup>50</sup> F. Rubio-Marcos, J. F. Fernandez, D. A. Ochoa, J. E. García, R. E. Rojas-Hernandez, M. Castro, and L. Ramajo, *J. Eur. Ceram. Soc.* **37**, 3501 (2017).